Trinuclear Clusters of Ruthenium-Containing Bridging and Ortho-Metalated 2,2′-Bis(diphenylphosphino)-1,1′-binaphthyl (BINAP): X-ray Structures of (*R*)-BINAP and $[Ru_3(\mu\text{-}OH)_2(CO)_8\{\mu\text{-}(R)\text{-BINAP}\}]$

Antony J. Deeming,* Despo M. Speel,† and Marc Stchedroff

Department of Chemistry, University College London, 20 Gordon Street, London WC1H 0AJ, U.K.

Received July 10, 1997[⊗]

The cluster $[Ru_3(CO)_{12}]$ normally reacts readily with tertiary phosphines and diphosphines in the presence of Me_3NO to give simple phosphine-substituted derivatives by a reaction involving nucleophilic attack of the amine oxide at CO leading to CO_2 formation. However, the corresponding reaction of $[Ru_3(CO)_{12}]$ with (*R*)-BINAP [2,2′-bis(diphenylphosphino)-1,1′-binaphthyl] in the presence of Me_3NO does not give $[Ru_3(CO)_{10}(BINAP)]$, as expected, but instead an 80% yield of the dihydroxy complex $[Ru_3(\mu\text{-}OH)_2(CO)_8\{\mu\text{-}(R)\text{-BINAP}\}]$ (**1**) as the first example of a μ-BINAP complex. NMR coalescence effects are observed in the ^1H NMR spectra, but by using a ^{13}CO-enriched sample, we were able to show that the fluxionality is not cluster-centered since the $^{13}C\{^1H\}$ NMR spectrum for the CO ligands is invariant over a wide temperature range. COSY spectra were used to show that there is restricted rotation about two of the four P−Ph bonds while the other two are rotating freely. From a single-crystal XRD study it can be seen that two Ph groups are unimpeded while the other two are closely aligned to the naphthyl rings in a graphitic manner and it is this that leads to the restricted rotation. This bridging ligand adopts quite a different conformation about the C−PPh_2 bonds to that in free BINAP, the structure of which was also determined for comparison, and somewhat different from that in known chelating BINAP complexes. In contrast, the direct thermal reaction of (*R*)-BINAP with $[Ru_3(CO)_{12}]$ in octane gives, in addition to traces of two uncharacterized species, a 38% yield of the cluster $[Ru_3(\mu\text{-}H)\{\mu\text{-}(R)\text{-BINAP-H}\}(CO)_9]$ (**2**), in which we believe that ortho metalation has occurred at one of the four Ph rings to form the first example of a cyclometalated BINAP ligand. We have been unable to obtain simple derivatives such as $[Ru_3(CO)_{11}(BINAP)]$ or $[Ru_3(CO)_{10}(BINAP)]$, although we have shown that the osmium analogues may be synthesized.

Introduction

The diphosphine ligand 2,2′-bis(diphenylphosphino)-1,1′-binaphthyl (BINAP)[1] is an example of a chiral binaphthyl compound which has found considerable use as a chiral auxiliary in transition-metal-catalyzed asymmetric synthesis.[2] Mononuclear BINAP ruthenium(II) and rhodium(I) complexes have been applied widely and successfully to enantioselective catalysis giving high enantiomer excesses in many cases. For example, the ruthenium(II) complexes $[Ru(RCO_2)_2(BINAP)]$ are excellent catalysts for asymmetric hydrogenation of various functionalised alkenes.[3] Similarly, the complex $[Rh(BINAP)(solvent)_2]^+$ is effective for asymmetric hydrogenation.[4] There is only evidence that catalysis by BINAP metal complexes involves mononuclear complexes which have BINAP as a chelating bidentate ligand.

Crystallographic studies have been carried out on BINAP complexes of various types, but all of these contain chelating bidentate BINAP. Some complexes contain one BINAP in a distorted square-planar arrangement: $[Rh(nbd)(BINAP)]ClO_4$,[5] $[PdCl_2(BINAP)]$,[6] $[Pt(o\text{-anisyl})_2(BINAP)]$,[7] and various allyl complexes of the type $[Pd(\eta^3\text{-allyl})(BINAP)]$.[8] Other BINAP complexes are octahedral or pseudo-octahedral: $[Ru(RCO_2)_2(BINAP)]$[9] and benzene or cyclopentadienyl complexes of ruthenium(II).[10] Three complexes contain-

* To whom correspondence should be addressed. E-mail: a.j.deeming@ucl.ac.uk.

† Despo M. Speel has published under her maiden name Despo M. Michaelidou.

⊗ Abstract published in *Advance ACS Abstracts,* December 1, 1997.

(1) (a) Miyashita, A.; Yasuda, A.; Takaya, H.; Toriumi, K.; Ito, T.; Souchi, T.; Noyori, R. *J. Am. Chem. Soc.* **1980**, *102*, 7932. (b) Takaya, H.; Akutagawa, S.; Noyori, R. *Org. Synth.* **1988**, *67*, 20.

(2) (a) Noyori, R. *Asymmetric Catalysis in Organic Synthesis*; Wiley: New York, 1994. (b) Noyori, R. *Acta Chem. Scand.* **1996**, *50*, 380. (c) Noyori, R in Trost, B. M., *Ed (IUPAC) Stereocontrolled Organic Synthesis*; Blackwell: Oxford, 1994, p 1. (d) G. Procter *Asymmetric Synthesis*, Oxford University Press: Oxford, 1996. (e) Noyari, R.; Takaya, H. *Acc. Chem. Res.* **1990**, *23*, 345.

(3) (a) Kitamura, M.; Tokunaga, M.; Noyori, R. *J. Org. Chem.* **1992**, *57*, 4053. (b) Takaya, H.; Ohta, T.; Inoue, S.; Tokunaga, M.; Kitamura, M.; Noyari, R. *Org. Synth.* **1993**, *72*, 74.

(4) Wang, X.; Bosnich, B. *Organometallics* **1994**, *13*, 4131.

(5) Toriumi, K; Ito, T.; Takaya, H.; Souchi, T.; Noyari, R. *Acta Crystallogr., Sect. B* **1982**, *38*, 807.

(6) Ozawa, F.; Kubo, A.; Matsumoto, Y.; Hayashi, T.; Nishioka, E.; Yanagi, K.; Moriguchi, K. *Organometallics* **1993**, *12*, 4188.

(7) (a) Alcock, N. W.; Brown, J. M.; Perez-Torrente, J. J. *Tetrahedron Lett.* **1992**, *33*, 389. (b) Brown, J. M.; Perez-Torrente, J. J.; Alcock, N. W. *Organometallics* **1995**, *14*, 1195.

(8) (a) Pregosin, P. S.; Ruegger, H.; Salzmann, R.; Albinati, A.; Lianzi, F.; Kunz, R. W. *Organometallics* **1994**, *13*, 83. (b) Pregosin, P. S.; Ruegger, H.; Salzmann, R.; Albinati, A.; Lianzi, F.; Kunz, R. W. *Organometallics* **1994**, *13*, 5040.

S0276-7333(97)00587-6 CCC: $14.00

ing two BINAP ligands have been structurally characterized: [Rh(BINAP)$_2$]ClO$_4$ is distorted square-planar,[11] [Pt(BINAP)$_2$] is tetrahedral,[12] while [RuHCl(BINAP)$_2$] is *trans* octahedral.[13] There are some known triruthenium complexes with BINAP ligands, but the X-ray structure of [Ru$_3$(μ_3-Cl)$_2$(μ-Cl)$_3${BINAP}$_3$]BF$_4$ shows that it is not a cluster but has three octahedral ruthenium(II) atoms linked by chloride bridges.[14] The BINAP ligands are chelating in the same way as in mononuclear ruthenium(II) complexes. The complex [Rh$_3$(μ_3-COD)$_2$(BINAP)$_3$]ClO$_4$ is related but contains square-planar rhodium(I) with chelating BINAP ligands.[15]

Prior to this work, the only known BINAP metal cluster appears to be [Ru$_4$(μ-H)$_4$(CO)$_{10}${(S)-BINAP}], formed by direct substitution of [Ru$_4$(μ-H)$_4$(CO)$_{12}$].[16] In this complex the diphosphine is chelating at one Ru atom of a tetrahedral Ru$_4$ cluster, so its coordination is basically no different to that in mononuclear complexes. There are no authenticated examples of BINAP coordinating other than as a bidentate ligand at a single metal atom. However, it has been pointed out that BINAP is a moderately flexible ligand that can coordinate to metal atoms of various sizes.[2b] We now discovered bridging BINAP as part of an 8-membered ring (this work) and monodentate BINAP in [Os$_3$(CO)$_{11}$(BINAP)].[17] These discoveries indicate the potential for using bridging BINAP in dinuclear and polynuclear compounds where the influence of the chiral ligand would extend over a group of metal atoms.

There have been many synthetic and structural studies on complexes of the type [Ru$_3$(CO)$_{10}$(diphosphine)],[18] [Ru$_3$(CO)$_8$(diphosphine)$_2$],[19] and [Ru$_3$(CO)$_6$(diphosphine)$_3$],[20] and in one case a chiral diphosphine has been used.[18h] However, it seems that trinuclear metal systems have not previously been studied with BINAP and here we report our work on triruthenium BINAP clusters. We set out to synthesise clusters with bridging BINAP such as 1,1- or 1,2-[Ru$_3$(CO)$_{10}$(BINAP)]. If such complexes could be made, it would be possible to examine chiral induction in the reactions of these clusters with prochiral organics, possibly leading to cluster catalysis. In particular we were interested to know whether the stereochemistry of reactions at the metal atoms *not* coordinated to BINAP might be controlled by the BINAP stereochemistry. It was not obvious that BINAP would bridge to give the 1,2-isomer rather than chelate to give the 1,1-isomer because bidentate ligands can coordinate in either way and isomers of [Os$_3$(CO)$_{10}$(diphosphine)] are known for some diphosphines. For example, the 1,1- and 1,2-isomers of [Os$_3$(CO)$_{10}$(Ph$_2$PCH$_2$CH$_2$PPh$_2$)] are formed by reaction of 1,1- or 1,2-[Os$_3$(CO)$_{10}$(C$_4$H$_6$)], where the buta-1,3-diene (C$_4$H$_6$) is either chelating or bridging,[21] although isomers of this kind have not been observed for ruthenium.

Since we were particularly keen to get high-yield syntheses, we chose to use the method of reacting [Ru$_3$(CO)$_{12}$] with BINAP in the presence of Me$_3$NO, a reagent which has been shown to be effective in oxidatively removing CO to allow phosphine coordination under very mild conditions. Remarkably, the product we obtained in good yield was not the expected [Ru$_3$(CO)$_{10}$(BINAP)] but rather a bis(hydroxy) Ru$_3$ cluster. Direct thermal reaction of BINAP with [Ru$_3$(CO)$_{12}$] gave ortho metallation of BINAP.

Scheme 1

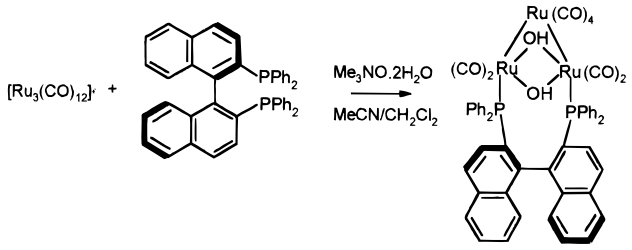

Results and Discussion

Synthesis and X-ray Characterization of the Cluster [Ru$_3$(μ-OH)$_2$(CO)$_8${μ-(*R*)-BINAP}]. The cluster [Ru$_3$(CO)$_{12}$] was reacted with (*R*)-BINAP in the presence of trimethylamine-*N*-oxide (Me$_3$NO·2H$_2$O) in the mixed solvent system methanol, acetonitrile, and dichloromethane under reflux for 1 h. In addition to some very minor uncharacterized products, we were able to separate a major product in 80%, as orange-brown crystals, which was shown to be the quite unexpected product [Ru$_3$(μ-OH)$_2$(CO)$_8${μ-(*R*)-BINAP}] (**1**) (Scheme 1). The crystals were coated with a sticky film which could not be washed off and this probably accounts for the C and H analytical data being rather higher than calculated (see the Experimental Section). FAB mass spectra are consistent with the formulation given. The ^{1}H NMR spectrum showed the expected spectrum in the phenyl and naphthyl region, consistent

(9) (a) Ohta, T.; Takaya, H.; Noyori, R. *Inorg. Chem.* **1988**, *27*, 566. (b) Ashby, M. T.; Khan, M. A.; Halpern, J. *Organometallics* **1991**, *10*, 2011.

(10) (a) Mashima, K.; Kusano, K.; Ohta, T.; Noyori, R. Takaya, H. *J. Chem. Soc., Chem. Commun.* **1989**, 1208. (b) Hoke, J. B.; Hollis, L. S.; Stern, E. W. *J. Organomet. Chem.* **1993**, *455*, 193. (c) Patak, D. D.; Adams, H.; Bailey, N. A.; King, P. J.; White, C. *J. Organomet. Chem.* **1994**, *479*, 237.

(11) Tani, K.; Yamagata, T.; Tatsumo, Y.; Yamagata, Y.; Tomita, K.; Akutagawa, S.; Kumobayashi, H; Otsuka, S. *Angew. Chem. Int. Ed. Engl.* **1985**, *24*, 217.

(12) Taninaga, H.; Sakai, K.; Tsubomura, T. *J. Chem. Soc., Chem. Commun.* **1995**, 2273.

(13) (a) Kawano, H.; Ikariya, T.; Ishii, Y.; Kodama, T.; Saburai, M.; Yoshikawa, S.; Uchida, Y.; Akutagawa, S. *Bull. Chem. Soc. Jap.* **1992**, *65*, 1595. (b) Kawano, H.; Ishii, Y.; Kodama, T.; Suburai, M.; Uchida, Y. *Chem. Lett.* **1987**, 1311.

(14) Mashima, K.; Hino, T.; Takaya, H. *J. Chem. Soc., Dalton Trans.* **1992**, 2099.

(15) Yamagata, T.; Tani, K.; Tatsuno, Y.; Saito, T. *J. Chem. Soc., Chem. Commun.* **1988**, 466.

(16) Braga, D.; Matteoli, U.; Sabatino, P.; Scrivanti, A. *J. Chem. Soc., Dalton Trans.* **1995**, 419.

(17) Deeming, A. J.; Stchedroff, M. Unpublished results.

(18) (a) Cabeza, J. A.; Riera, V.; Jeannin, Y.; Miguel, D *Inorg. Chim. Acta* **1990**, *168*, 77. (b) Bartsch, R.; Gelessus, A.; Hitchcock, P. B.; Nixon, J. F. *J. Organomet. Chem.* **1992**, *430*, C10. (c) Teoh, S.-G.; Fun, H.-K.; bin Shawkataly, O. *Z. Kristallogr.* **1990**, *190*, 287.; (d) Coleman, A. W.; Jones, D. F.; Dixneuf, P. H.; Brisson, C.; Bonnet, J.-J.; Lavigne, G. *Inorg. Chem.* **1984**, *23*, 952. (e) Harding, M. M.; Maginn, S. J.; Smith, A. K. *Acta Crystallogr., Sect. C* **1988**, *44*, 237. (f) Shiu, K.-B.; Peng, S.-M.; Cheng, M.-C. *J. Organometal. Chem.* **1993**, *453*, 133. (g) Gallucci, J. C.; Gilbert, K. B.; Hsu, W.-L.; Shore, S. G. *Cryst. Struct. Commun.* **1982**, *11*, 1385. (h) Evans, J.; Jones, A. G.; Webster, M. *Acta Crystallogr., Sect. C* **1989**, *45*, 595. (i) Chacon, S. T.; Cullen, W. R.; Bruce, M. I.; bin Shawkataly, O.; Einstein, F. W. B.; Jones, R. H.; Willis, A. C. *Can. J. Chem.* **1990**, *68*, 2001. (j) Shen, H.; Bott, S. G.; Richmond, M. G. *Organometallics* **1995**, *14*, 4625.

(19) (a) Field, J. S.; Haines, R. J.; Jay, J. A. *J. Organomet. Chem.* 1989, 377, C35. (b) Lavigne, G.; Bonnet, J.-J. *Inorg. Chem.* **1981**, *20*, 2713. (c) Lavigne, G.; Lugan, N.; Bonnet, J.-J. *Acta Crystallogr., Sect. B* **1982**, *38*, 1911.

(20) Mirza, H. A.; Vittal, J. J.; Puddephatt, R. J. *Inorg. Chem.* **1993**, *32*, 1327.

(21) Deeming, A. J.; Donovan-Mtunzi, S.; Hardcastle, K. I.; Kabir, S. E.; Henrick, K.; McPartlin, M. *J. Chem. Soc., Dalton Trans.* **1988**, 579.

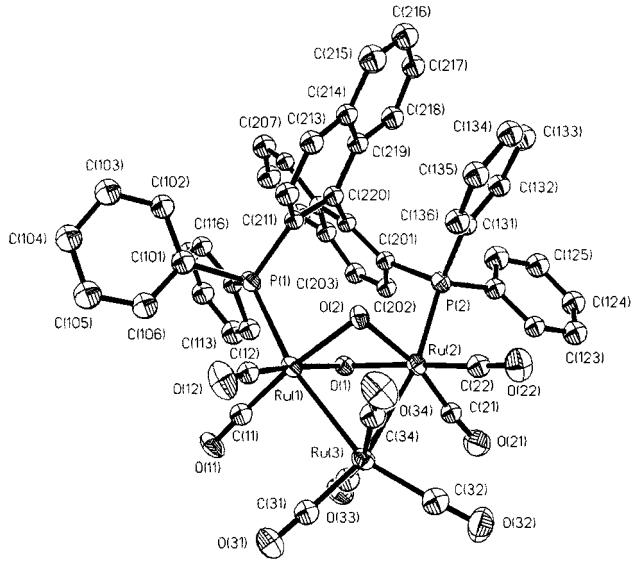

Figure 1. Molecular structure of $[Ru_3(\mu\text{-}OH)_2(CO)_8\{\mu\text{-}(R)\text{-}BINAP\}]$ (**1**) showing the crystallographic labeling scheme. Thermal ellipsoids are at the 30% probability level.

with C_2 symmetry, although some of the signals were extremely broad at room temperature (see below). A high-field triplet at δ −1.48 (2H), showing equal coupling to both ^{31}P nuclei (J = 4.0 Hz), is not in the correct shift range for hydride. However, μ-hydroxy ^{1}H NMR signals have been reported at δ −1.08 for $[Os_3(\mu\text{-}OH)\{\mu\text{-}SC(NMe_2)_2\}(\mu\text{-}MeOCO)(CO)_9]$,[22] at δ −1.61 for $[Os_3(\mu\text{-}H)(\mu\text{-}OH)(CO)_9(PMe_2Ph)]$,[23] at δ 0.54 for $[Os_3(\mu\text{-}H)(\mu\text{-}OH)(CO)_9(PEt_3)]$,[24] at δ 0.44 for $[Os_3(\mu\text{-}H)(\mu\text{-}OH)(CO)_8(dppm)]$,[24] at δ 0.20 for $[Os_3(\mu\text{-}H)(\mu\text{-}OH)(CO)_{10}]$,[25] and at δ −1.63, −1.30, and −1.48 for various PPh_3-substituted derivatives of this compound.[25] Therefore it seems likely that **1** is a dihydroxy complex. The ^{31}P-$\{^1$H$\}$ NMR singlet is also consistent with C_2 symmetry as for BINAP itself. In addition, the cluster was characterized by IR spectra, FAB MS (parent molecular ion observed), and single-crystal X-ray diffraction.

Single crystals of **1** were grown by slow diffusion of 2-methoxyethanol into a dichloromethane solution, the structure determined is shown in Figure 1, and selected bond lengths and angles are given in Table 1. Each of the two independent but very similar molecules, A and B, in the unit cell (Z = 8) contain isosceles triangles of ruthenium atoms with the unique longer nonbonded Ru···Ru edge bridged by (*R*)-BINAP and two OH ligands. The unbridged Ru−Ru distances are 2.814(3) and 2.820(2) Å (mol. A), and 2.810(3) and 2.812(2) Å (mol. B), while the Ru···Ru distances are 3.023(2) Å (mol. A) and 3.030(2) Å (mol. B). Compound **1** is a 50-electron cluster, and as expected, has only two Ru−Ru bonds. We believe that the Ru···Ru distance is as short as this to accommodate the two OH bridges, since the distance is similar to those in related triruthenium clusters with double alkoxy bridges for which Ru···Ru distances are in the range 3.002−3.072 Å.[26] Therefore the Ru···Ru distance in **1** is probably controlled by the OH bridges and may not be optimal for BINAP bridging.

Table 1. Selected Bond Lengths (Å) and Angles (deg) for 1

molecule A		molecule B	
Ru(1)−O(2)	2.102(13)	Ru(4)−O(4)	2.112(12)
Ru(1)−O(1)	2.111(13)	Ru(4)−O(3)	2.118(13)
Ru(1)−P(1)	2.391(6)	Ru(4)−P(3)	2.400(6)
Ru(1)−Ru(3)	2.814(3)	Ru(4)−Ru(6)	2.810(3)
Ru(1)−Ru(2)	3.023(2)	Ru(4)−Ru(5)	3.030(2)
Ru(2)−O(1)	2.102(13)	Ru(5)−O(3)	2.111(14)
Ru(2)−O(2)	2.133(14)	Ru(5)−O(4)	2.124(13)
Ru(2)−P(2)	2.394(6)	Ru(5)−P(4)	2.403(6)
Ru(2)−Ru(3)	2.820(2)	Ru(5)−Ru(6)	2.812(2)
P(1)−C(101)	1.79(2)	P(3)−C(311)	1.83(2)
P(1)−C(211)	1.84(2)	P(3)−C(301)	1.86(2)
P(1)−C(111)	1.82(2)	P(3)−C(401)	1.86(2)
P(2)−C(131)	1.81(2)	P(4)−C(331)	1.83(2)
P(2)−C(121)	1.82(2)	P(4)−C(411)	1.84(2)
P(2)−C(201)	1.85(2)	P(4)−C(321)	1.86(2)
O(2)−Ru(1)−O(1)	79.1(5)	O(4)−Ru(4)−O(3)	79.5(5)
O(2)−Ru(1)−P(1)	87.7(4)	O(4)−Ru(4)−P(3)	90.2(4)
O(1)−Ru(1)−P(1)	89.7(4)	O(3)−Ru(4)−P(3)	88.7(4)
Ru(3)−Ru(1)−Ru(2)	57.65(6)	Ru(6)−Ru(4)−Ru(5)	57.43(6)
O(1)−Ru(2)−O(2)	78.6(5)	O(3)−Ru(5)−O(4)	79.4(5)
O(1)−Ru(2)−P(2)	88.3(4)	O(3)−Ru(5)−P(4)	89.1(4)
O(2)−Ru(2)−P(2)	90.2(4)	O(4)−Ru(5)−P(4)	88.6(4)
Ru(3)−Ru(2)−Ru(1)	57.44(6)	Ru(6)−Ru(5)−Ru(4)	57.34(6)
Ru(1)−Ru(3)−Ru(2)	64.91(6)	Ru(4)−Ru(6)−Ru(5)	65.23(6)
Ru(2)−O(1)−Ru(1)	91.7(5)	Ru(5)−O(3)−Ru(4)	91.5(5)
Ru(1)−O(2)−Ru(2)	91.1(5)	Ru(4)−O(4)−Ru(5)	91.3(5)

Because the structure of BINAP has not been reported, we determined its structure for comparison with the known structures of chelating BINAP and this unique structure of bridging BINAP. Two projections of the molecular structure of (*R*)-BINAP are shown in Figure 2, and selected bond lengths and angles are given in Table 2. The dihedral angle between the two naphthyl groups in free BINAP is 88.3°, compared with 78.1° in **1**, and the values typically found for chelating BINAP are in the range 65−77°. In contrast to coordinated BINAP, there is freedom to rotate about the naphthyl−PPh_2 bonds, and the observed conformation reduces the lone pair−lone pair repulsions and is therefore not preorganized to coordinate either as a chelating or bridging ligand. The orientation of the phosphorus lone pairs was assessed by placing a ghost H-atom on each phosphorus in an idealized position with all HPC angles equal. The torsional angle H−P(1)−P(2)−H was calculated to be 165.8°. The corresponding angle in **1** is the torsional angle Ru(1)−P(1)−P(2)−Ru(2), which is 1.9°, which is close to zero as expected. There needs to be an approximately 90° rotation about each naphthyl−PPh_2 bond of free BINAP to set up the correct conformation for coordination.

The other major difference between free, chelating, and bridging BINAP is the P(1)···P(2) distance, which is 4.218 Å in free (*R*)-BINAP and 4.719 Å in **1**. Typically this distance is lower in chelating than in free BINAP; for example, the P···P distance in $[PdCl_2(BINAP)]$[6] is 3.249 Å. This shortening on chelation results from the need to attain normal metal−phosphorus distances within the chelate ring, while the lengthening on bridging results from the requirement to redirect the

(22) Azam, K. A.; Dilshad, R.; Kabir, S. E.; Miah, R.; Shahiduzzaman, M.; Rosenberg, E.; Hardcastle, K. I.; Hursthouse, M. B.; Malik, K. M. A. *J. Clust. Chem.* **1996**, *7*, 49.

(23) Ditzel, E. J.; Gomez-Sal, M. P.; Johnson, B. F. G.; Lewis, J.; Raithby, P. R. *J. Chem. Soc.,* Dalton Trans. **1987**, 1623.

(24) Hodge, S. R.; Johnson, B. F. G.; Lewis, J.; Raithby, P. R. *J. Chem. Soc., Dalton Trans.* **1987**, 931.

(25) Ho, W. G.-Y.; Wong, W. T. *Polyhedron* **1995**, *14*, 2849.

(26) (a) Bhaduri, S.; Sapre, N.; Khwaja, H.; Jones, P. G. *J. Organomet. Chem.* **1992**, *426*, C12. (b) Bohle, D. S.; Breidt, V. F.; Powell, A. K.; Vahrenkamp, H. *Chem. Ber.* **1992**, *125*, 1111. (c) Santini, C. C.; Basset, J.-M.; Fontal, B.;Krause, J.; Shore, S.; Charrier, C.; *J. Chem. Soc., Chem. Commun.* **1987**, 512. (d) van Doorn, J. A.; van Leeuwen, P. W. N. M. *J. Organomet. Chem.* **1981**, *222*, 299.

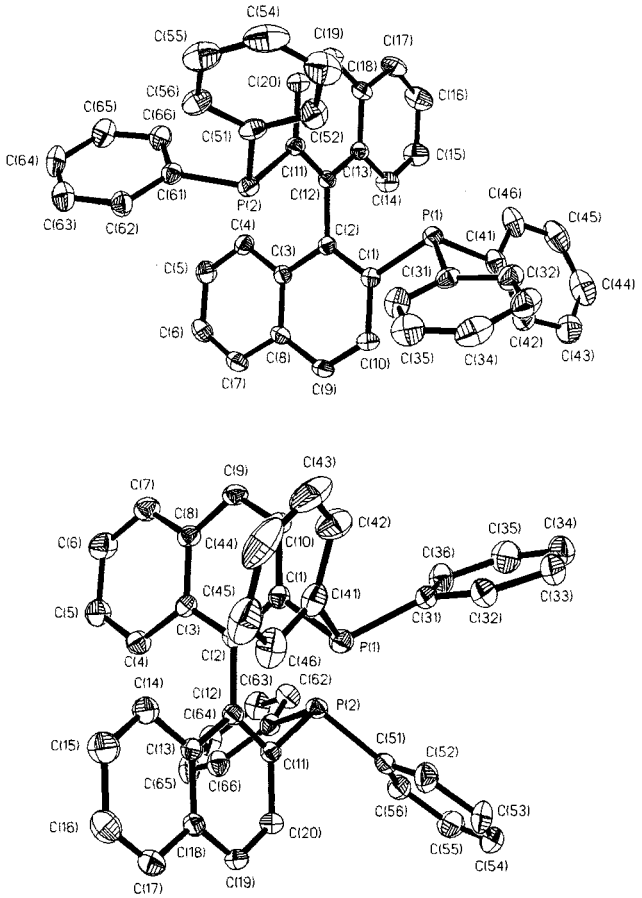

Figure 2. Two projections of the structure of (*R*)-BINAP showing the crystallographic labeling scheme. Thermal ellipsoinds are at the 30% probability level.

Table 2. Selected Bond Lengths (Å) and Angles (deg) for (*R*)-BINAP

P(1)−C(31)	1.819(5)	P(2)−C(11)	1.843(5)
P(1)−C(1)	1.830(5)	C(1)−C(2)	1.375(7)
P(1)−C(41)	1.843(6)	C(2)−C(12)	1.499(6)
P(2)−C(61)	1.823(6)	C(11)−C(12)	1.380(7)
P(2)−C(51)	1.839(5)		
C(31)−P(1)−C(1)	103.5(2)	C(51)−P(2)−C(11)	100.6(2)
C(31)−P(1)−C(41)	103.3(3)	C(2)−C(1)−P(1)	118.7(4)
C(1)−P(1)−C(41)	101.4(2)	C(10)−C(1)−P(1)	122.1(4)
C(61)−P(2)−C(51)	102.3(3)	C(12)−C(11)−P(2)	118.7(4)
C(61)−P(2)−C(11)	102.1(2)	C(20)−C(11)−P(2)	121.7(4)

phosphorus lone pairs toward the metal centers. The Ph groups in chelating BINAP (Figure 3b) are clearly either equatorial or axial, providing the mechanism for transmission of asymmetry from the binaphthyl group toward the other ligands at the metal center, an essential feature for achieving high enantiomer excesses in asymmetric catalysis. Similar effects are apparent in μ-BINAP (Figure 3c), although the equatorial Ph groups are drawn away from adjacent ligands in this case. The difference between chelating and bridging BINAP results directly from the angle between the P−M vectors being about 90° in Figure 3b but only 41.5° in Figure 3c.

In addition to these changes on coordination, there are significant differences in the conformation of the PPh_2 groups and in the approach of Ph to naphthyl groups. In free BINAP the Ph groups are distant from the naphthyl groups, but the process of rotating about Ph_2P−naphthyl bonds to achieve coordination results in one phenyl of each PPh_2 aligning in a parallel

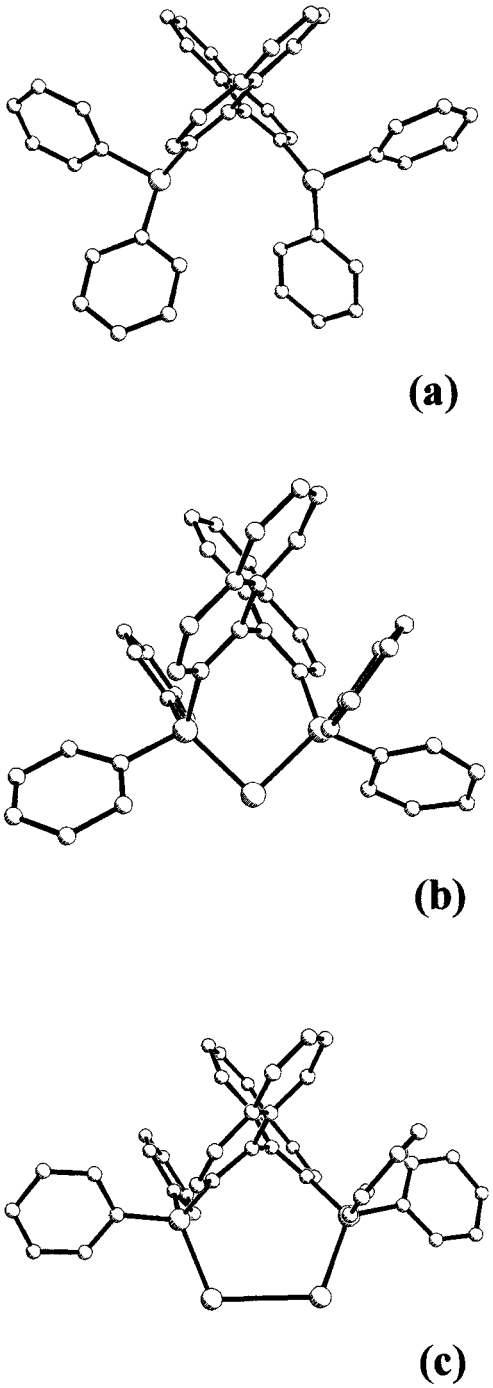

Figure 3. Structures of BINAP: (a) uncomplexed, (b) chelating in [$PdCl_2$(BINAP)], and (c) bridging in cluster **1**.

graphitic manner to the naphthyl group to which the PPh_2 is not bonded directly. This parallel alignment is also found in μ-BINAP, as seen in the space-filling picture of **1** in Figure 4, and has a marked effect on the barrier to phenyl rotation.

Fluxionality of 1. Figure 5 shows the variable-temperature ^{1}H NMR spectra of **1**. The OH signal is essentially temperature-independent and the ^{13}C NMR for the CO ligands and the ^{31}P{^{1}H} NMR spectra likewise. The ^{13}C{^{1}H} NMR spectrum of a ^{13}CO-enriched sample of **1** contains the expected four signals associated with C_2 symmetry: δ 206.5 (s), 205.9 (s), 205.4 (s), and 198.6 (d, $J_{PC} = 4.0$ Hz), the doublet being best assigned to the carbonyls d in Figure 6, which are *trans* to the ^{31}P nuclei across the bonding Ru−Ru edges.

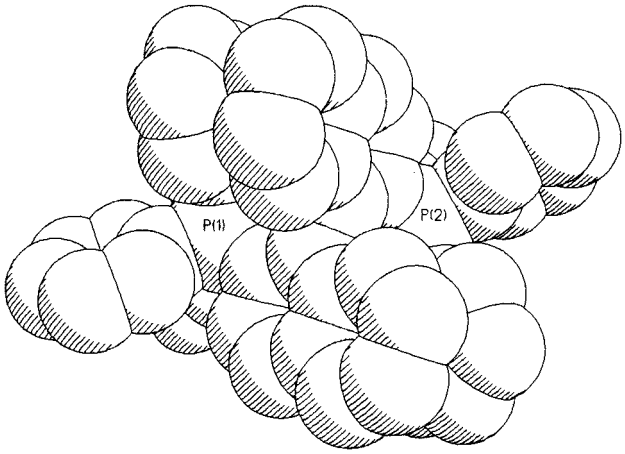

Figure 4. Space-filling model of BINAP in **1**. The $Ru_3(OH)_2(CO)_8$ group of atoms are almost totally obscured. Rotation (B) of the phenyl groups closely parallel to the naphthyl groups is severely restricted, while there is no evidence for restricted rotation of the other phenyl groups (A).

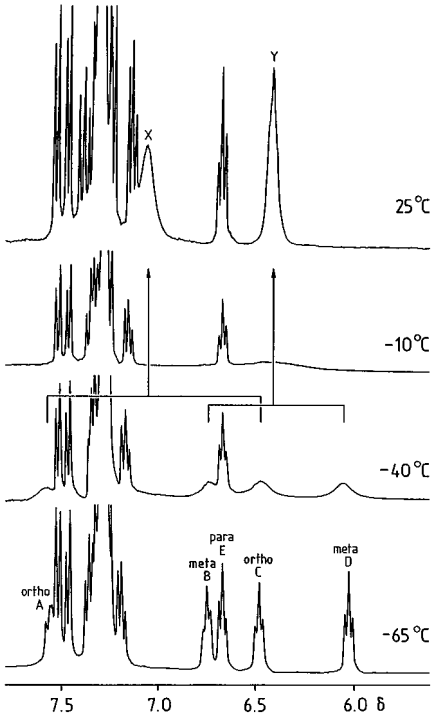

Figure 5. ^{1}H NMR spectra of **1** in $CDCl_3$ showing the pairwise coalescence of *ortho* phenyl signals (A and C) and *meta* phenyl signals (B and D) and temperature invariance of *para* signal E. The freely rotating phenyl signals appear at δ 7.2−7.4.

This spectrum does not change noticably between −65 and 40 °C, indicating that the observed coalescence in the ^{1}H spectrum is not the result of fluxionality in the $M_3(CO)_{10}$ framework. Analysis of a COSY ^{1}H NMR spectrum at −65 °C showed that the exchange was occurring between protons giving signals A and C to give X and between B and D to give Y and that the coupling is entirely consistent with two equivalent Ph groups giving rise to signals A−E, that is, these two phenyl groups have nonequivalent *ortho* and *meta* positions as a result of restricted rotation at low temperature. Exchange is between nonequivalent 2 and 6 positions and between 3 and 5 positions as a result of restricted rotation about two of the four Ph−P bonds. This can be rationalized by unrestricted rotation (A) and restricted rotation (B) (Figure 4). We are assuming that it is the phenyls that lie parallel to the naphthyl groups that experience the greatest barrier to rotation. To our knowledge restricted phenyl rotation of this kind has not been reported for chelating BINAP, although Figure 3 shows that this is a possibility.

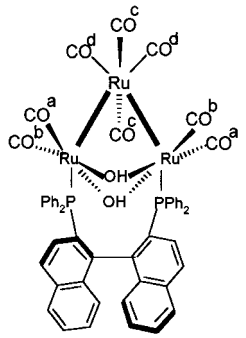

Figure 6. Structure of **1** showing the labeling of the CO ligands.

Origin of the Hydroxy Ligands in 1. Oxide or hydroxide ligands are commonly found in osmium and ruthenium clusters and are normally derived, sometimes adventitiously, from water or dioxygen.[22,25] In this case there is the alternative that the hydroxide ligands are derived from trimethylamine *N*-oxide. We have not carried out labeling experiments to confirm this. It is remarkable that no $[Ru_3(CO)_{10}(BINAP)]$ at all is formed and that the yield of **1** is 80%, considering the considerable use that has been made of the $[Ru_3(CO)_{12}]$/tertiary phosphine/Me_3NO system in preparing substituted derivatives of the trinuclear carbonyl. The only possible related report is the formation of $[Os_3(\mu\text{-OH})(\mu\text{-MeOCO})\{\eta^1\text{-}(Me_2N)_2CS\}(CO)_9]$ (10%) in the $[Os_3(CO)_{12}]$/tetramethylurea/$Me_3NO{\cdot}2H_2O$ reaction in methanol/benzene, but even here the major product (50%) is the substituted derivative $[Os_3(CO_{11})\{\eta^1\text{-}(Me_2N)_2\text{-}CS\}]$.[22]

Reaction of $[Ru_3(CO)_{12}]$ with (*R*)-BINAP in the Absence of Me_3NO. Direct thermal reaction of the carbonyl with (*R*)-BINAP is slow, but in refluxing octane a complex of apparent formula $[Ru_3(CO)_9(BINAP)]$ (**2**) is formed in 38% yield along with small amounts of two uncharacterized products, one mauve and one yellow, which are not $[Ru_3(CO)_x(BINAP)]$ (x = 10 or 11). The double doublet signal at δ −16.49 in the ^{1}H NMR spectrum established that **2** is a hydrido cluster. Successive decoupling of the two ^{31}P NMR signals at δ 26.92 and 42.16 established that the hydride signal was a double doublet as a result of coupling to two nonequivalent ^{31}P nuclei. The $^{13}C\{H\}$ NMR spectrum is extremely complex, showing over 20 signals (doublets and multiplets), and confirmed that the BINAP ligand had lost C_2 symmetry (as does the ^{31}P NMR spectrum), as would be expected for orthometalation. We propose that **2** is the cluster $[Ru_3(\mu\text{-H})\{\mu_3\text{-}(C_6H_4)PPhC_{20}H_{12}PPh_2\}\text{-}(CO)_9]$, which would be the first example of an orthometalated BINAP complex. The orange solid did not produce crystals of suitable quality for X-ray diffraction studies, so we are unable to propose a structure, but we suggest that metalation of one phenyl group has occurred to give a μ_3-ligand. Attempts to carbonylate **2** to give $[Ru_3(CO)_{10}(BINAP)]$ by bubbling CO through refluxing octane or decane solutions were unsuccessful.

Table 3. Crystal Data for 1 and (*R*)-BINAP

	1	(*R*)-BINAP
cryst size (mm)	0.35 × 0.25 × 0.18	0.46 × 0.43 × 0.40
formula	$C_{52}H_{34}O_{10}P_2Ru_3$	$C_{44}H_{32}P_2$
Fw	1183.94	622.64
color	red	colorless
cryst system	ortho rhombic	monoclinic
space group	$P2_12_12_1$	$P2_1$
Temp (K)	293(2)	293(2)
a (Å)	17.982(5)	9.151(3)
b (Å)	23.775(4)	18.783(5)
c (Å)	24.262(9)	10.036(4)
β (deg)	90	103.11(3)
V (Å^3)	10372(5)	1680.0(9)
Z	8	2
d_{calc} (g cm^{-3})	1.516	1.231
μ(Mo Kα) (mm^{-1})	0.978	0.160
F(000)	4704	652
2*θ* range (deg)	5−45	5−50
no. rflns measd	7289	3205
no. indep rflns	7288	3016
wR2 (all data)	0.2218	0.1320,
R1 [$I>2\sigma(I)$]	0.0690	0.0492
goodness-of-fit on F^2	1.049	1.073
Data/parameters	7284/687	3012/414
Absolute structure parameter	0.0(2)	0.05(9)
Largest diff peak/hole (eÅ^{-3})	1.344, −0.800	0.225, −0.254

The only product was the mauve uncharacterized compound from the original preparation (identical IR spectra).

Experimental Section

Materials. The cluster [$Ru_3(CO)_{12}$] and (*R*)-BINAP were used as obtained from Aldrich. The 400 MHz NMR spectra were obtained on a Varian VXR400 spectrometer, ^{31}P-decoupled ^{1}H NMR spectra on a Bruker Spectrospin AC200 spectrometer, IR spectra on a Nicolet 280 FTIR spectrometer, and FAB MS (MNBA matrix) on a ZAB mass spectrometer.

Reaction of [$Ru_3(CO)_{12}$] with (*R*)-BINAP in the Presence of $Me_3NO{\cdot}2H_2O$. Solid samples of ruthenium carbonyl (0.050 g) and (*R*)-BINAP (0.070 g) were finely ground together and added to a solution of trimethylamine *N*-oxide (0.050 g) in methanol (1 mL) and acetonitrile (5 mL). Dichloromethane (35 mL) was added and the mixture refluxed under nitrogen for 1 h. The resulting solution was passed through a short column of silica (1 mL) to remove any excess of amine oxide and the solvent was removed under reduced pressure. The residual solid was separated by TLC on silica (Merck 5715 prepared plates) eluting with a dichloromethane−hexane mixture (3:7 v/v). The main orange-brown band was extracted with dichloromethane to yield [$Ru_3(\mu$-OH)$_2$(CO)$_8${μ-(*R*)-BINAP}] (**1**) as an orange-brown solid (80%). Spectral characterization: IR, *ν*(CO)/cm^{-1} (CH_2Cl_2): 2066(m), 2028(m), 2017(vs), 1986(w), 1972(w), 1937(s), 1911(vs); ^{1}H NMR ($CDCl_3$, −65 °C): exchanging Ph signals (broad above −65 °C), *δ* 6.03 (t, *meta*), 6.48 (t, *ortho*), 6.67 (t, *para*), 6.76 (t, *meta*), 7.56 (dd, *ortho*); other signals, *δ* 7.35−7.48 (overlapping m), 7.47 (d), 7.52 (d), −1.48 (OH, J_{PH} 4.0 Hz); ^{13}C{^{1}H} NMR ($CDCl_3$, 20 °C): CO signals (^{13}CO-enriched sample) *δ* 206.5 (s), 205.9 (s), 205.4 (s), 198.6 (d, J = 35.3 Hz), Ph and naphthyl signals, *δ* 143.6−126.6. ^{31}P{^{1}H} NMR ($CDCl_3$, 20 °C): *δ* 40.22 (s) (relative to $P(OMe)_3$). The parent molecular ion centered at 1184 Da and successive loss of 5CO were observed in the FAB MS. Anal. Calcd for $C_{52}H_{34}O_8P_2Ru_3$: C, 54.22; H, 2.98. Found: C, 55.59; H, 4.72.

Direct Thermal Reaction of [$Ru_3(CO)_{12}$] with (*R*)-BINAP. A mixture of ruthenium carbonyl (0.030 g) and (*R*)-BINAP (0.030 g) in octane (15 mL) was heated under nitrogen under reflux for 45 min. The cooled solution was filtered through a short silica column and the solvent was removed under reduced pressure (10^{-3} mm Hg) to give a brown residue. This was dissolved in CH_2Cl_2, loaded on to TLC plates (SiO_2), and eluted with a dichloromethane/hexane mixture (3:7 by volume) to give three bands. Two of the bands gave small amounts of uncharacterized material, a mauve residue (0.004 g) and a yellow residue (0.001 g), while the main orange-brown band gave an orange solid (0.23 g, 38%) characterized as [Ru_3-(μ-H)(μ_3-BINAP-H)(CO)$_9$] (**2**). Anal. Calcd for $C_{53}H_{32}O_9P_2$-Ru_3: C, 54.04; H, 2.74. Found: C, 54.81; H, 3.22. Spectral characterization: IR, *ν*(CO)/cm^{-1} (hexane): 2065(vs), 2027(vs), 2014(vs), 1985(s), 1970(s), 1962(m), 1948(m); ^{1}H NMR ($CDCl_3$, 25 °C): *δ* 8.26 (m), 7.69 (d), 7.55−7.49 (m), 7.40 (dd), 7.30−7.20 (m), 7.09 (dd), 7.05 (t), 6.90 (t), 6.84 (m), 6.82 (m), 6.78 (d), 6.66 (dd), 6.53 (d), 6.40 (dd), 6.37 (m), 6.33 (d), 6.28 (t), 6.19 (t), −16.49 (dd, J_{PH} = 14.0, 42.5 Hz, Ru*H*Ru); ^{13}C{^{1}H} NMR ($CDCl_3$, 20 °C): CO signals, *δ* 202.9 (s), 202.8 (s), 202.7 (s), 198.2 (s), other signals at 168.7 (d), 150.1 (d), 144.0 (s) and about 40 signals (doublets and singlets, *δ* 123 to 138). ^{31}P-{^{1}H} NMR ($CDCl_3$, 25 °C): *δ* 42.1 (dd, J_{PP} = 40, J_{HP} = 43 Hz), 26.8 (dd, J_{PP} = 40, J_{HP} = 14 Hz). The highest mass peaks observed in the FAB MS correspond to the loss of 2CO from [Ru_3(μ-H)(μ_3-BINAP-H)(CO)$_9$].

X-ray Crystallographic Studies of 1 and (*R*)-BINAP. Single crystals of **1** were obtained by overlaying a saturated CH_2Cl_2 solution with ethanol and allowing solvent diffusion to occur at room temperature. Single crystals of (*R*)-BINAP were obtained by evaporation of a 2-ethoxyethanol solution. Crystals were mounted on glass fibers on a Nicolet R3m/v diffractometer. Data were collected at 293(2) K using graphite-monochromated Mo-Kα radiation (*λ* = 0.71073 Å). Three standard reflections were measured every 97 reflections and showed very small variations in intensity. Intensities were corrected for Lorentz and polarization effects and empirical absorption corrections were applied for **1**, but not for (*R*)-BINAP, based upon Ψ-scans. Some details of the data collection and refinement are given in Table 3. Further details are provided in the Supporting Information. The structures were solved by direct methods and the structures refined by full-matrix least-squares refinement of $|F^2|$, using SHELXTL-PLUS. H-atoms were included in calculated positions using a riding model with a C−H distance of 0.96 Å and fixed isotropic thermal parameters of 0.08 Å^2. All other atoms were refined anisotropically except the carbon atoms in **1** which contained two independent molecules in the unit cell.

Acknowledgment. We are grateful to financial support from the EPSRC and to Peter Grebenik (Oxford Brooks University) for the use of the Bruker AC200 for multinuclear decoupling experiments.

Supporting Information Available: Full listings of crystal data and structure refinement, fractional atomic coordinates, thermal parameters, and bond lengths and angles (24 pages). Ordering information is given on any current masthead page.

OM970587Z